ORGANOMETALLICS

Volume 2, Number 9, September 1983

Metal Cluster Nitrile Derivatives

J. K. Kouba and E. L. Muetterties*

Department of Chemistry, University of California, Berkeley, California 94720

M. R. Thompson and V. W. Day*

Department of Chemistry, University of Nebraska, Lincoln, Nebraska 68588

Received February 7, 1983

Thermal and photochemical activation of $Fe_3(\mu_3\text{-}PC_6H_5)_2(CO)_9$ and $Co_4(\mu_4\text{-}PC_6H_5)_2(CO)_{10}$, in acetonitrile or propionitrile solutions, provided the reactive nitrile clusters: $Fe_3(\mu_3\text{-}PC_6H_5)_2(CO)_8(NCR)$, $Fe_3(\mu_3\text{-}PC_6H_5)_2(CO)_7(NCR)_2$, and $Co_4(\mu_4\text{-}PC_6H_5)_2(CO)_9(NCR)$. Using these nitrile derivatives, a series of substitution derivatives with PF_3, $P(OR)_3$, PR_3, and AsR_3 ligands were prepared in high yield. Interestingly, the bis(acetonitrile) derivative of the iron cluster had both nitrile groups on the same (basal) iron atom. X-ray crystallographic studies for single crystals of $Fe_3(\mu_3\text{-}PC_6H_5)_2(CO)_7(NCCH_3)_2$ established that they utilize the centrosymmetric orthorhombic space group *Pnma*—C_{2h}^{16} with a = 13.103 (2) Å, b = 16.972 (2) Å, c = 25.038 (5) Å, and Z = 8. The asymmetric unit contains two crystallographically independent molecules both of which possess rigorous C_s-m symmetry. The molecular structure of $Fe_3(\mu_3\text{-}PC_6H_5)_2(CO)_7(NCCH_3)_2$ is related to that of the parent $Fe_3(\mu_3\text{-}PC_6H_5)_2(CO)_9$ with two of the equatorial carbonyl ligands on a single basal Fe atom replaced by acetonitrile ligands. Basically, the stereochemistry of the phosphorus- and arsenic-based ligand derivatives of the iron cluster were analogous to that of the parent nitrile derivatives from which they were obtained. Conformationally, there were differences that can be rationalized in terms of steric and electronic factors and of fluxional features of the molecules. Studies of the temperature-dependent ^{13}C spectra of the parent ion cluster and its derivatives established certain dominant mechanistic pathways for ligand site exchange in the cluster.

Introduction

Molecular metal clusters, often prepared under thermally rigorous conditions, are isolated typically as coordinately saturated molecules. These clusters generally will not react with other molecules until sufficient thermal or photochemical activation is supplied to break a bond. In metal carbonyl clusters, the *average* metal–metal and metal–carbonyl bond energies are comparable, and thus, in some cases, such clusters react by fragmentation, especially clusters based on 3d metals, while in other cases by M–CO bond scission.

To circumvent the problem of cluster fragmentation, we have attempted to synthesize reactive clusters, particularly clusters in which reactivity is associated with two or more metal centers. Two approaches to generating reactive clusters have been described. Preparation of coordinately unsaturated clusters has proven to be an effective approach[1] but one possibly limited in scope. Alternatively, clusters may be prepared with one or more relatively weak metal–ligand bonds. This tack has been successfully utilized by the Lewis–Johnson group[2a–c] and by the Shapley[3] group particularly with the labile ligand, a nitrile (with a terminal metal–nitrogen bond).[4] We have extended this approach to the generation of reactive nitrile derivatives of $Fe_3(\mu_3\text{-}PC_6H_5)_2(CO)_9$ and $Co_4(\mu_4\text{-}PC_6H_5)_2(CO)_{10}$ and describe here their preparation, structure, dynamic stereochemistry and chemistry. We also note here that a nitrile can function as a triply bridging ligand with the nitrile C and N atoms bonding to the metal atoms as established in the seminal studies of Andrews, Knobler,

(1) Muetterties, E. L. *Catal. Rev.—Sci. Eng.* **1981**, *23*, 69.

(2) (a) Johnson, B. F. G.; Lewis, J.; Nelson, W. J. H.; Puga, J.; Raithby, P. R.; Shröder, M.; Whitmire, K. H. *J. Chem. Soc., Chem. Commun.* **1982**, 610. (b) Johnson, B. F. G.; Lewis, J.; Pippard, D. A. *J. Chem. Soc., Dalton Trans.* **1981**, 407. (c) Dawson, P. A.; Johnson, B. F. G.; Lewis, J.; Puga, J.; Raithby, P. R.; Rosales, M. J. *Ibid.* **1982**, 233.

(3) (a) Tachikawa, M.; Shapley, J. R. *J. Organomet. Chem.* **1977**, *124*, C19. (b) Churchill, M. R.; Hollander, F. J.; Shapley, J. R.; Foose, D. S. *J. Chem. Soc., Chem. Commun.* **1978**, 534.

(4) (a) There are clusters that have one or more transition-metal atoms in combination with copper atoms in which the copper ligand is acetonitrile.[4b,c] (b) Albano, V. G.; Braga, D.; Martinengo, S.; Chini, P.; Sansoni, M.; Strumolo, D. *J. Chem. Soc., Dalton Trans.* **1980**, 52. (c) Bradley, J. S.; Pruett, R. L.; Hill, E.; Ansell, G. B.; Leonowicz, M. E.; Modrick, M. A. *Organometallics* **1982**, *1*, 748.

0276-7333/83/2302-1065$01.50/0

and Kaesz[5a] of $Fe_3(CO)_9(\mu_3\text{-}\eta^2\text{-}NCCH_2CH_2CH_3)$. Andrews et al.[5b,c] also showed a modeling of nitrile reductions using $Fe_3(CO)_9(\mu_3\text{-}\eta^2\text{-}NCCH_2CH_2CH_3)$ as have Mays and coworkers for an osmium cluster.[5d]

Experimental Section

Synthesis of $Fe_3(PC_6H_5)_2(CO)_9$. Following a modification of the Lampin and Mathey procedure[6], $Na_2Fe(CO)_4\cdot{}^3/_2C_4H_8O_2$ (20.0 g, 58 mmol) was slurried in 300 mL of dry tetrahydrofuran. Iron pentacarbonyl (8.0 mL, 59 mmol) dissolved in 100 mL of dry tetrahydrofuran was added to the slurry. The resultant orange slurry of $Na_2Fe_2(CO)_8$ was stirred for 1 h. To this slurry was added dropwise over 2 h 8.0 mL (59 mmol) of $C_6H_5PCl_2$ in 100 mL of dry tetrahydrofuran. After the mixture was stirred overnight at 25 °C, the solvent was removed by evacuation. The resultant residue was extracted with 500 mL of hot hexane. The cooled extract was reduced by half in volume by evacuation and then chromatographed on silica (3 × 30 cm, hexane). The deep red eluent was collected until it turned dark brown. The eluent was reduced by evacuation to about 200 mL in volume and rechromatographed on silica (3 × 30 cm, hexane). On the second column, the first red band was more clearly resolved and was collected. Solid appeared as the eluent was reduced in volume by evacuation. At this point, the solid was redissolved by heating and crystallized by cooling to −20 °C for several hours. The red crystals of $Fe_3(PC_6H_5)_2(CO)_9$ (2.9 g, 13%) were collected by filtration in air: $^{31}P\{^1H\}$ NMR (toluene) −319.9 ppm (s); mass spectrum, *m/e* 636 [$^{12}C_{21}{}^1H_{10}{}^{56}Fe_3{}^{16}O_9{}^{31}P_2$], 608, 580, 552, 524, 496, 468, 440, 412, 384 [P − *n*CO, *n* = 1–9]; IR (toluene solution) ν_{CO} 2041 (s), 2018 (s), 2003 (m), 1991 (m^{-1}, reported[7] 2046 (s), 2025 (s), 2009 (m), 1997 (w) cm^{-1}. Anal. Calcd for $C_{21}H_{10}Fe_3O_9P_2$: C, 39.67; H, 1.59; P, 9.74. Found: C, 39.58; H, 1.74; P, 9.65.

Synthesis of $Fe_3(PC_6H_5)_2(CO)_8(NCCH_3)$. A solution of $Fe_3(PC_6H_5)_2(CO)_9$ (1.0 g, 1.57 mmol) in 40 mL of dry CH_3CN was heated to reflux conditions for 8 h. The solvent was removed by evacuation, and the residue was redissolved in a mixture of 4 mL of hexane, 4 mL of toluene, and 3 mL of acetonitrile. This solution was placed onto a silica gel column (3 × 30 cm, hexane) and eluted with hexane until all unreacted $Fe_3(PC_6H_5)_2(CO)_9$ had been removed. Passage of a 3:1 hexane–toluene mixture containing 5% acetonitrile down the column developed a red band which was collected. This left a small residue of the bis(acetonitrile) complex on the column. The deep red-orange solution was evaporated to dryness in vacuum. The residue was redissolved in dry CH_3CN, and the resultant solution was filtered and then reduced to less than 5 mL in volume. Cooling of the solution of −20 °C led to the formation of deep red, clustered crystals which were collected by filtration (272 mg, 27%): $^{31}P\{^1H\}$ NMR (toluene) −318.7 and −298.9 ppm (AB pattern, J_{AB} = 287 Hz); mass spectrum, *m/e* 608 [$^{12}C_{22}{}^1H_{13}{}^{56}Fe_3{}^{14}N^{16}O_8{}^{31}P_2$ − CH_3CN], 580, 552, 524, 496, 468, 440, 412, 384 [P − CH_3CN − *n*CO, *n* = 1–8], 41 [$^{12}C_2{}^1H_3{}^{14}N$]; IR (toluene solution) ν_{CO} 2053 (m), 2008 (s), 1998 (s), 1974 (b, w), 1957 (b, w) cm^{-1}. Anal. Calcd for $C_{22}H_{13}Fe_3NO_8P_2$: C, 40.72; H, 2.02; N, 2.16; P, 9.55. Found: C, 40.83; H, 2.18; N, 2.26; P, 9.57.

Synthesis of $Fe_3(PC_6H_5)_2(CO)_8(NCCH_2CH_3)$. A solution of $Fe_3(PC_6H_5)_2(CO)_9$ (1.0 g, 1.57 mmol) in 30 mL of dry propionitrile was heated to reflux conditions for 2 h after which the solvent was removed by evacuation. The resultant residue was dissolved in a mixture of 2 mL of propionitrile and 8 mL of hexane, and this solution was placed onto a silica gel column (3 × 30 cm, hexane). Unreacted $Fe_3(PC_6H_5)_2(CO)_9$ was removed by elution with hexane. Then elution with a 3:1 hexane–toluene containing 5% propionitrile developed a red band which was collected. Solvent was removed from this fraction by evacuation. The product was recrystallized by dissolution in 3 mL of propionitrile, followed by addition of 50 mL of heptane, reduction of the final solution volume by half, and cooling to −20 °C for 12 h. The red crystals (325 mg, 31%) were collected by filtration: $^{31}P\{^1H\}$ NMR (toluene) −319.1 and −298.8 ppm (AB pattern, J_{AB} = 285 Hz); IR (toluene solution) ν_{CO} 2053 (m), 2008 (s), 1998 (s), 1974 (b, w), 1957 (b, w) cm^{-1}. Anal. Calcd for $C_{23}H_{15}Fe_3NO_8P_2$: C, 41.68; H, 2.28; N, 2.11; P, 9.35. Found: C, 42.09; H, 2.52; N, 2.12; P, 8.92.

Synthesis of $Fe_3(PC_6H_5)_2(CO)_8[P(OCH_3)_3]$. A solution of $Fe_3(PC_6H_5)_2(CO)_9$ (1.0 g, 1.57 mmol) in 35 mL of dry CH_3CN was heated to reflux for 8 h. After the solvent was removed by evacuation, the residue was redissolved in 25 mL of toluene. This solution was treated with trimethyl phosphite (1.0 mL, 8.48 mmol), stirred for 2 days, and then taken to dryness by evacuation. Chromatography of the residue on silica (3 × 30 cm, 3:1 hexane–toluene) yielded starting material first and then the product second. The latter fraction was evacuated to dryness. The residue was recrystallized from hexane to give red needles (480 mg, 42%): ^1H NMR (toluene-d_8) δ 3.2 (d, J_{PH} = 12.1 Hz) and 3.6 (d, J_{PH} = 11.9 Hz); $^{31}P\{^1H\}$ NMR (1:1 toluene–tetrahydrofuran, −60 °C) −180.0 (t), −299.9 ppm (d) (A_2X pattern, J_{PP} = 45 Hz); mass spectrum, *m/e* 732 [$^{12}C_{23}{}^1H_{19}{}^{56}Fe_3{}^{16}O_{11}{}^{31}P_2$], 704, 676, 648, 620, 592, 564, 536, 508 [P − *n*CO, *n* = 1–8]; IR (toluene solution) ν_{CO} 2055 (m), 2013 (s), 1998 (s), 1977 (b) cm^{-1}, reported[7] 2059 (m), 2019 (s), 1998 (s), 1970 (m) cm^{-1}. Anal. Calcd for $C_{23}H_{19}Fe_3O_{11}P_3$: C, 37.75; H, 2.62; P, 12.70. Found: C, 37.72; H, 2.72; P, 12.44.

Synthesis of $Fe_3(PC_6H_5)_2(CO)_8[As(C_6H_5)_3]$. A solution of $Fe_3(PC_6H_5)_2(CO)_8(CH_3CN)$ (200 mg, 0.31 mmol) and $As(C_6H_5)_3$ (1.0 g, 3.27 mmol) in 20 mL of toluene was stirred for 2 days. The solvent was removed by evacuation and the residue chromatographed on Florisil (3 × 30 cm, 1:1 toluene–hexane). The major band was collected and evaporated to dryness. Recrystallization of the residue from CH_2Cl_2–heptane gave 149 mg (52%): $^{31}P\{^1H\}$ NMR (1:1 toluene-d_8–tetrahydrofuran, −40 °C) −298.3 ppm (s); mass spectrum, *m/e* 608 [$^{12}C_{38}{}^1H_{25}{}^{75}As^{56}Fe_3{}^{16}O_8{}^{31}P_2$ − $As(C_6H_5)_3$], 580, 552, 524, 496, 468, 440, 412, 384 [P − $As(C_6H_5)_3$ − *n*CO, *n* = 1–8], 306 $^{12}C_{18}{}^1H_{15}{}^{75}As$], IR (toluene solution) ν_{CO} 2052 (m), 2011 (s), 1999 (s) cm^{-1}. Anal. Calcd for $C_{38}H_{25}AsFe_3O_8P_2$: C, 49.93; H, 2.76; P, 6.78. Found: C, 49.77; H, 2.91; P, 6.62.

Synthesis of $Fe_3(PC_6H_5)_2(CO)_8[P(C_6H_5)_3]$. A 200-mg (0.31-mmol) sample of $Fe_3(PC_6H_5)_2(CO)_9$ was placed into 25 mL of dry CH_3CN and was heated to reflux for 8 h. The solvent was removed by evacuation and the residue redissolved in 25 mL of toluene. This solution was then treated with 1.0 g (3.82 mmol) of triphenylphosphine, stirred for 24 h, and then evacuated to dryness. Chromatography of the residue on silica (3 × 30 cm, 1:1 hexane–toluene) yielded starting material first and then a red band of the product. This latter fraction was evaporated to dryness and then recrystallized from CH_2Cl_2–heptane to give 126 mg (45%): $^{31}P\{^1H\}$ NMR (1:1 toluene–tetrahydrofuran solution, −60 °C) −72 (t), −291 ppm (d) (A_2X pattern, J_{PP} = 30 Hz); mass spectrum, *m/e* 608 [$^{12}C_{38}{}^1H_{25}{}^{56}Fe_3{}^{16}O_8{}^{31}P_3$ − $P(C_6H_5)_3$], 580, 552, 524, 496, 468, 440, 412, 384 [P − $P(C_6H_5)_3$ − *n*CO, *n* = 1–8]; IR (toluene solution) ν_{CO} 2054 (m), 2028 (w), 2014 (s), 1997 (s), 1974 (b) cm^{-1}. Anal. Calcd for $C_{38}H_{25}Fe_3O_8P_3$: C, 52.46; H, 2.90; P, 10.68. Found: C, 52.22; H, 3.12; P, 10.48.

Synthesis of $Fe_3(PC_6H_5)_2(CO)_8(PF_3)$. $Fe_3(PC_6H_5)_2(CO)_8(CH_3CN)$ (200 mg, 0.31 mmol) and 15 mL of toluene were placed in a sealable vessel, the tube was cooled and evacuated, and then approximately 1.5 mmol of PF_3 was condensed into the vessel. The vessel was sealed and stirred for 24 h. After the seal was broken, the solvent was removed by evacuation. Recrystallization of the residue from hexane gave 110 mg (0.16 mmol, 51%) of $Fe_3(PC_6H_5)_2(CO)_8(PF_3)$ which was recrystallized from hexane to give red crystals of analytical purity: $^{31}P\{^1H\}$ NMR (1:1 toluene-d_8–tetrahydrofuran, −40 °C) −319 (s), −174 (q, J_{PF} = 1289 Hz), −325 and −172 ppm (A_2B part of A_2BX_3 pattern, J_{AB} = 35.5 Hz, J_{AX} = 10.7 Hz, J_{BX} = 1306 Hz); ^{19}F NMR (1:1 toluene-d_8–tetrahydrofuran, −20 °C) −174 (d, J_{PF} = 1289 Hz) and −166 ppm (dt, J_{P_AF} = 10.7 Hz, J_{P_BF} = 1306 Hz); mass spectrum, *m/e* 696 [$^{12}C_{20}{}^1H_{10}{}^{19}F_3{}^{56}Fe_3{}^{16}O_8{}^{31}P_3$], 668, 640, 612, 584, 556, 528, 500 (P − *n*CO, *n* = 1–7], 608, 580, 552, 524, 496, 468, 440, 412, 384 [P − PF_3 − *n*CO, *n* = 1–8]; IR (toluene solution) ν_{CO} 2068 (m), 2037

(5) (a) A very different structural and electronic class of nitrile derivatives of clusters has been reported by: Andrews, M. A.; Knobler, C. B.; Kaesz, H. D. *J. Am. Chem. Soc.* **1979**, *101*, 7260 for $Fe_3(\mu_3\text{-}\eta^2\text{-}NCCH_2CH_2CH_3)(CO)_9$ in which the CN functionality bridges the three iron atoms and both the carbon and nitrogen atoms are bonded to iron atoms. (b) Andrews, M. A.; Kaesz, H. D. *J. Am. Chem. Soc.* **1977**, *99*, 6763. (c) Andrews, M. A.; Van Buskirk, G.; Nobler, C. B.; Kaesz, H. D. *Ibid.* **1979**, *101*, 7245. (d) Banford, J.; Dawood, Z.; Henrick, K.; Mays, M. J. *J. Chem. Soc., Chem. Commun.* **1982**, 554–555 for $(\mu\text{-}H)_2Os_3(\mu_3\text{-}NCH_2CF_3)(CO)_9$ with the nitrogen atom bridging a face of Os_3 triangular core.

(6) Lampin, J.; Mathey, F. *C.R. Frances Acad. Sci., Ser. C* **1976**, *282*, 979.

(7) Treichel, P. M.; Dean, W. K.; Douglas, W. M. *Inorg. Chem.* **1972**, *11*, 1609.

(s), 2005 (s) cm^{-1}. Anal. Calcd for $C_{20}H_{10}F_3Fe_3O_8P_3$: C, 34.53; H, 1.45; P, 13.36. Found: C, 34.77; H, 1.53; P, 13.08.

Reaction of $Fe_3(PC_6H_5)_2(CO)_8(NCCH_2CH_3)$ with Anhydrous HCl. A solution of $Fe_3(PC_6H_5)_2(CO)_9$ (200 mg, 0.31 mmol) in 25 mL of dry propionitrile was heated to reflux for 2 h and then the solvent was removed by evacuation. The residue was dissolved in 30 mL of toluene and the resultant solution saturated with hydrogen chloride by passing this gas through the solution. The flask was sealed and stirred at room temperature for 12 h during which time the solution lightened considerably in color and a small amount of white solid precipitated. The solution was taken to dryness by evacuation. Thin-layer chromatography of the residue (silica, 4:1 hexane–toluene) showed two major components, a fast moving yellow compound and a slow moving compound which was identified as $Fe_3(PC_6H_5)_2(CO)_8(NCCH_2CH_3)$. The yellow compound was purified by chromatography on silica (2 × 20 cm, 9:1 hexane–toluene), recrystallized from hexane (90 mg, 58%), and identified as the previously reported $Fe_2(PHC_6H_5)_2(CO)_6$:[7] ^1H NMR (benzene-d_6) δ 3.8 (d, J_{PH} = 300 Hz), 6.9 (m) and 7.5 (m); mass spectrum, m/e 498 [$^{12}C_{18}{}^1H_{12}{}^{56}Fe_2{}^{16}O_6{}^{31}P_2$], 470, 442, 412, 386, 358, 330 [P – nCO, n = 1–6]; IR (hexane solution) ν_{CO} 2064 (m), 2029 (s), 1999 (m), 1989 (m) cm^{-1}, reported[7] 2063 (s), 2027 (s), 2000 (sh), 1996 (s), 1984 (s) cm^{-1}. Anal. Calcd for $C_{18}H_{12}Fe_2O_6P_2$: C, 43.42; H, 2.43; P, 12.44. Found: C, 43.11; H, 2.61; P, 12.31.

Synthesis of $Fe_3(PC_6H_5)_2(CO)_7(NCCH_3)_2$. A solution of $Fe_3(PC_6H_5)_2(CO)_9$ (1.0 g, 1.57 mmol) dissolved in 150 mL of dry acetonitrile was photolyzed for 2 h at 0 °C by using an Ace Glass medium-pressure mercury vapor lamp apparatus. During the course of the photolysis, the solution turned from orange-red to deep red and evolved carbon monoxide. The reaction mixture was evacuated to dryness. The residue was dissolved in a mixture of 4 mL of hexane, 4 mL of toluene, and 3 mL of acetonitrile and was chromatographed on silica (3 × 30 cm, hexane). Elution with hexane removed unreacted $Fe_3(PC_6H_5)_2(CO)_9$. Elution with 3:1 hexane–toluene plus 5% acetonitrile removed several minor products from the column. The major product was eluted from the column with 1:1 hexane–toluene plus 5% acetonitrile. This fraction was evacuated to dryness. The residue was redissolved in 30 mL of dry acetonitrile, filtered, reduced in volume until crystals appeared, and then cooled to −20 °C for several hours. The resultant dark red needles were collected by filtration (256 mg, 25%): $^{31}P\{^1H\}$ NMR (CD_3CN, 20 °C) −285.5 ppm (s); IR (toluene solution) ν_{CO} 2039 (m), 1998 (s), 1984 (m), 1964 (m), 1925 (m) cm^{-1}. Anal. Calcd for $C_{23}H_{16}Fe_3N_2O_7P_2$: C, 41.74; H, 2.44; N, 4.23; P, 9.36. Found: C, 40.93; H, 2.38; N, 3.80; P, 9.80.

Synthesis of $Fe_3(PC_6H_5)_2(CO)_7[P(OCH_3)_3]_2$. $Fe_3(PC_6H_5)_2(CO)_7(NCCH_3)_2$ (256 mg, 0.39 mmol), $P(OCH_3)_3$ (0.5 mL, 4.24 mmol), and 25 mL of toluene were stirred for 24 h at room temperature. The solvent was removed by evacuation and the residue chromatographed on silica (3 × 30 cm, 1:1 toluene–hexane). The major band was collected and the solution evacuated to dryness. The residue was recrystallized from 4:1 hexane–toluene to give 172 mg (54%). $^{31}P\{^1H\}$ NMR (toluene-d_8–tetrahydrofuran, −40 °C) −162.0 (ddd, J_1 = 49.2 Hz, J_2 = 49.3 Hz, J_3 = 57.5 Hz), −184.4 (ddd, J_1 = 21.3 Hz, J_2 = 49.2 Hz, J_3 = 57.6 Hz), −297.2 ppm (m); mass spectrum, m/e 828 [$^{12}C_{25}{}^1H_{28}{}^{56}Fe_3{}^{16}O_{13}{}^{31}P_4$], 800, 772, 744, 716, 688, 660, 632 [P – nCO, n = 1–7]; IR (toluene solution) ν_{CO} 2044 (m), 2001 (s) 1984 (m) 1968 (m) cm^{-1}. Anal. Calcd for $C_{25}H_{28}Fe_3O_{13}P_4$: C, 36.27; H, 3.41; P, 14.96. Found: C, 36.22; H, 3.48; P, 15.28.

Synthesis of ^{13}CO-Enriched $Fe_3(PC_6H_5)_2(CO)_9$. A solution of $Fe_3(PC_6H_5)_2(CO)_8(NCCH_3)$ (500 mg, 0.78 mmol) dissolved in 15 mL of toluene was freeze–thaw degassed and then sealed under 15 mL of ^{13}CO at 600 mm pressure. After 2 days at room temperature, ^{13}CO was added to the tube to bring the pressure back up to 600 mm. The same procedure was repeated after 2 more days. Two days following, the solution was taken to dryness by evaucation and the residue chromatographed on silica (3 × 30 cm, hexane). The ^{13}CO-enriched complex was recrystallized from hexane (274 mg, 56%): ^{13}C NMR (1:1 toluene–tetrahydrofuran, −60 °C) −214.4 (s, 3 C), −213.7 (t, J_{PC} = 9.5 Hz, 2 C), −206.4 ppm (s, 4 C), (1:1 toluene–tetrahydrofuran, 70 °C) −213.7 (s, 3 C) −208.2 ppm (s, 6 C); mass spectrum, parent envelope m/e (relative intensity) 634 (3.9), 635 (18.2), 636 (28.7), 637 (100.0), 638 (42.0), 639 (11.3, calcd for 15.5% $(^{13}CO)_0$, 69.2% $(^{13}CO)_1$, 15.3% $(^{13}CO)_2$, m/e (relative intensity) 634 (4.0), 635 (18.7), 636 (29.5), 637 (100.0), 638 (42.0), 639 (9.1).

In a manner analogous to that described above, 256 mg (0.39 mmol) of $Fe_3(PC_6H_5)_2(CO)_7(NCCH_3)_2$ was reacted with ^{13}CO in toluene to give the ^{13}CO-enriched complex: ^{13}C NMR (1:1 toluene–tetrahydrofuran, −40 °C) identical with that described above; mass spectrum, parent envelope m/e (relative intensity) 634 (1.3), 635 (5.3), 636 (21.9), 637 (41.0), 638 (100.0), 639 (47.2), 640 (11.2), calcd for 2.0% $(^{13}CO)_0$, 20.7% $(^{13}CO)_1$, 60.4% $(^{13}CO)_2$, 16.9% $(^{13}CO)_3$, m/e (relative intensity) 634 (1.7), 635 (6.6), 636 (21.7), 637 (40.4), 638 (100.0), 639 (46.9), 640 (10.2).

Synthesis of ^{13}CO-Enriched $Fe_3(PC_6H_5)_2(CO)_8(NCC_2H_5)$. ^{13}CO-enriched $Fe_3(PC_6H_5)_2(CO)_8(NCC_2H_5)$ was prepared by a procedure identical with that described above using ^{13}CO-enriched $Fe_3(PC_6H_5)_2(CO)_9$: ^{13}C NMR (1:1 toluene–tetrahydrofuran, −60 °C) −218.2 (dd, J_{PC} = 10 Hz, $J_{P'C}$ = 16 Hz), −216.6 (s), −215.8 (m) −210.6 (dd, J_{PC} = 18 Hz, $J_{P'C}$ = 31 Hz), −209.5 ppm (t, J_{PC} = 19 Hz), (1:1 toluene–tetrahydrofuran, 60 °C) −217.5 (dd, J_{PC} = 10 Hz, $J_{P'C}$ = 16 Hz), −216.2 (s), −210.9 (s), −210.2 ppm (dd, J_{PC} = 18 Hz, $J_{P'C}$ = 31 Hz).

Synthesis of ^{13}CO-Enriched $Fe_3(PC_6H_5)_2(CO)_7(NCCH_3)_2$. This ^{13}CO-enriched complex was prepared by a procedure identical with that described above by using ^{13}CO-enriched $Fe_3(PC_6H_5)_2(CO)_9$: ^{13}C NMR (1:1 toluene–tetrahydrofuran, −60 °C) −216.1 (t, J_{PC} = 18 Hz), −211.7 (s), −211.0 (b), −205.0 ppm (s), (1:1 toluene–tetrahydrofuran, 60 °C) −215.6 (t, J_{PC} = 18 Hz), −211.6 (s), −206.5 ppm (s).

Synthesis of ^{13}CO-Enriched $Fe_3(PC_6H_5)_2(CO)_8[P(OCH_3)_3]$. This ^{13}CO-enriched complex was prepared by a procedure identical with that described above by using ^{13}CO enriched $Fe_3(PC_6H_5)_2(CO)_9$: ^{13}C NMR (1:1 toluene–tetrahydrofuran, −60 °C) −219.4 (s), −218.9 (s), −212.6 (d, J_{PC} = 17 Hz), −211.3 ppm (s), (1:1 toluene–tetrahydrofuran, 60 °C) −218.3 (s), −213.3 (s), −212.6 ppm (d, J_{PC} = 17 Hz).

Synthesis of $Co_4(PC_6H_5)_2(CO)_{10}$. Following the procedure described by Ryan and Dahl,[8] 10.0 g (157 mmol) of zinc dust was placed in a Schlenk tube which was evacuated and flame dried. Upon cooling, a stir bar, 100 mL of dry toluene, and 5.0 g (14.6 mmol) of $Co_2(CO)_8$ were added to the tube. The tube was sealed and stirred at ambient temperature in the dark for 12 h. The reaction mixture was then filtered. To the filtered supernatent was added 2.0 mL (14.7 mmol) of $C_6H_5PCl_2$ in 50 mL of dry toluene, dropwise, over 1 h. The mixture was heated to reflux for 6 h. The cooled reaction mixture was filtered through Celite in air, and the filtrate was evacuated to dryness. The residue was dissolved in 100 mL of acetone and poured into 75 mL of water. The resultant red precipitate was filtered onto Celite, and the filtrate was discarded. The collected solids were redissolved in acetone which was filtered and then taken to dryness. The residue was chromatographed in air on silica (2 × 20 cm, toluene). The resultant red eluent was reduced in volume by half and cooled to −20 °C from which, after 12 h, 750 mg (14%) of deep red crystals were collected by filtration. Mass spectrum, m/e 732 [$^{12}C_{22}{}^1H_{10}{}^{59}Co_4{}^{16}O_{10}{}^{31}P_2$], 704, 676, 648, 620, 592, 564, 536, 508, 480, 452 [P – nCO, n = 1–10]; IR (toluene solution) ν_{CO} 2043 (s), 2031 (s), 2018 (s), 1978 (b), 1879 (m) cm^{-1}, reported[6] 2040 (s), 2032 (s), 2016 (s), 1866 (m) cm^{-1}. Anal. Calcd for $C_{22}H_{10}Co_4O_{10}P_2$: C, 36.10; H, 1.38; P, 8.46. Found: C, 35.84; H, 1.58; P, 8.42.

Synthesis of $Co_4(PC_6H_5)_2(CO)_9(NCCH_3)$. A solution of $Co_4(PC_6H_5)_2(CO)_{10}$ (200 mg, 0.27 mmol) was suspended in 50 mL of dry acetonitrile and refluxed for 2 h. Deoxygenated water (30 mL) was added dropwise to the cooled solution causing the precipitation of a red crystalline solid. The crystals (120 mg, 60%) were collected by filtration and dried under vacuum: IR (acetonitrile solution) ν_{CO} 2014 (w), 2025 (m), 2006 (s), 1986 (sh), 1830 (b) cm^{-1}. Anal. Calcd for $C_{23}H_{15}Co_4NO_9P_2$: C, 37.08; H, 1.76; N, 1.88; P, 8.31. Found: C, 37.20; H, 2.15; N, 2.18; P, 8.10.

Synthesis of $Co_4(PC_6H_5)_2(CO)_9[P(OCH_3)_3]$. $Co_4(PC_6H_5)_2(CO)_{10}$ (200 mg, 0.27 mmol) was suspended in 40 mL of dry acetonitrile which was then heated to reflux for 2 h. After removal of the solvent by evacuation and dissolution of the residue in 25 mL of dry toluene, 0.1 mL (0.85 mmol) of trimethyl phosphite was added to the reaction mixture. After 3 h of stirring, the

(8) Ryan, R. C.; Dahl, L. F. *J. Am. Chem. Soc.* **1975**, *97*, 6904.

solution had turned from deep red-brown to bright red. The solvent was removed by evacuation, and the residue was chromatographed on silica (2 × 20 cm, 1:1 toluene–hexane). The major red band was collected, and the solution was evacuated to dryness. The residue was recrystallized from CH_2Cl_2–heptane to give red crystals. Mass spectrum, *m/e* 828 [$^{12}C_{24}{}^{1}H_{19}{}^{59}Co_4{}^{16}O_{12}{}^{31}P_3$], 800, 772, 744, 716, 688, 660, 632, 604, 576, [P – *n*CO, *n* = 1–9], 704, 676, 648, 620, 592, 564, 536, 508, 480, 452 [P – $P(OCH_3)_3$ – *n*CO, *n* = 0–9]; IR (toluene solution) ν_{CO} 2058 (w), 2025 (s), 2011 (s), 2001 (s), 1864 (b) cm^{-1}. Anal. Calcd for $C_{24}H_{19}Co_4O_{12}P_3$: C, 34.81; H, 2.31; P, 11.22. Found: C, 34.80; H, 2.57; P, 11.77.

Synthesis of $Co_4(PC_6H_5)_2(CO)_8[P(OCH_3)_3]_2$. $Co_4(PC_6H_2)_2(CO)_9[P(OCH_3)_3]$ (100 mg, 0.12 mmol), dissolved in 30 mL of dry acetonitrile, was heated to reflux for 3.5 h. After removal of the solvent by evacuation and dissolution of the residue in 25 mL of dry toluene, 0.15 mL (1.27 mmol) of trimethyl phosphite was added to the reaction mixture. After 24 h the solvent was removed by evacuation and the residue chromatographed on silica (2 × 20 cm, 1:1 toluene–hexane). The major red band was collected and evacuated to dryness. The residue was recrystallized from CH_2Cl_2–heptane: IR (toluene solution) ν_{CO} 2041 (w), 2009 (s), 1988 (s), 1844 (m) cm^{-1}. Anal. Calcd for $C_{26}H_{28}Co_4O_{14}P_4$: C, 33.78; H, 3.05; P, 13.40. Found: C, 33.55; H, 3.25; P, 13.18.

Synthesis of $Co_4(PC_6H_5)_2(CO)_9[P(C_6H_5)_3]$. Method A. $Co_4(PC_6H_5)_2(CO)_{10}$ (85 mg, 0.11 mmol) and $P(C_6H_5)_3$ (30 mg, 0.11 mmol) were dissolved in toluene and heated to reflux for 3 h. The solvent was removed by evacuation, and the residue was chromatographed on silica (2 × 20 cm, toluene). The major band was collected and evacuated to dryness. The red-brown residue was recrystallized from CH_2Cl_2–heptane: IR (toluene solution) ν_{CO} 2048 (w), 2014 (s), 1998 (m), 1984 (w) cm^{-1}. Anal. Calcd for $C_{39}H_{25}Co_4O_9P_3$: C, 48.48; H, 2.61; P, 9.62. Found: C, 48.64; H, 2.90; P, 9.45.

Method B. $Co_4(PC_6H_5)_2(CO)_{10}$ (200 mg, 0.27 mmol) was dissolved in dry CH_3CN which was heated to reflux for 2 h. The solvent was removed by evacuation, and $P(C_6H_5)_3$ (200 mg, 0.76 mmol) and 30 mL of toluene were added to the residue. After the solution was stirred at room temperature for 12 h, the solvent was removed by evacuation and the residue chromatographed on silica (2 × 20 cm, toluene). The major band was collected and evaporated to dryness. The residue was recrystallized from CH_2Cl_2–heptane: IR (toluene solution) ν_{CO} 2046 (m), 2010 (s), 2000 (w), 1996 (m), 1983 (w), 1835 (w) cm^{-1}. Anal. Calcd for $C_{39}H_{25}Co_4O_9P_2$: C, 48.48; H, 2.61; P, 9.62. Found: C, 48.45; H, 2.84; P, 9.56.

X-ray Crystallographic Study[9] of $Fe_3(\mu_3\text{-}PC_6H_5)_2(CO)_7(NCCH_3)_2$. Large well-shaped dark red single crystals of $Fe_3(\mu_3\text{-}PC_6H_5)_2(CO)_7(NCCH_3)_2$, **3**, obtained as described above by recrystallization from acetonitrile, are at 20 ± 1 °C, orthorhombic with a = 13.103 (2) Å, b = 16.972 (2) Å, c = 25.038 (5) Å, V = 5568 (1) Å^3, and Z = 8 (μ_a(Mo K$\bar{\alpha}$)[10] = 1.70 mm^{-1}; d_{calcd} = 1.580 g cm^{-3}; d_{obsd} = 1.591 g cm^{-3} measured by flotation in aqueous KI solution). The systematically absent reflections in the diffraction pattern were those required by the centrosymmetric space group *Pnma*—D_{2h}^{16} (No. 62)[11a] or the noncentrosymmetric space group $Pn2_1a$ [an alternate setting of $Pna2_1$—C_{2v}^{9} (No. 33)[11b]]. The choice of centrosymmetric space group *Pnma* was fully supported by the various statistical indictors based on normalized structure factors as well as by all stages of the subsequent structure determination and refinement.

Intensity measurements were made on a Nicolet P$\bar{1}$ autodiffractometer by using 1.0°-wide ω scans and graphite-monochromated Mo K$\bar{\alpha}$ radiation for a parallelepiped-shaped specimen with dimensions of 0.42 × 0.50 × 0.58 mm. This crystal was glued to the end of a thin glass fiber and mounted on the goniometer head with its long axis nearly parallel to the ϕ axis of the diffractometer. A total of 6494 independent reflections having $2\theta_{MoK\bar{\alpha}}$ < 54.9° were measured with a scanning rate of 3°/min in two concentric shells of increasing 2θ, each containing approximately 3250 reflections. The data collection and reduction procedures which were used are described in ref 12.

The six Fe atoms of the two crystallographically independent molecules which comprise the asymmetric unit of **3** were located by using "direct methods" (MULTAN). These Fe atoms were then used to calculate a difference Fourier synthesis which revealed the remaining non-hydrogen atoms of the asymmetric unit. Unit-weighted full-matrix least-squares refinement which utilized anisotropic thermal parameters for all non-hydrogen atoms converged to R_1 (unweighted, based on F)[13] = 0.038 and R_2 (weighted, based on F)[13] = 0.040 for 2415 independent reflections having $2\theta_{MoK\bar{\alpha}}$ < 43° and $I > 3\sigma(I)$. A difference Fourier synthesis calculated at this point revealed the 16 hydrogen atoms in chemically anticipated positions. All additional least-squares cycles for **3** refined hydrogen atoms with isotropic thermal parameters and non-hydrogen atoms with anisotropic thermal parameters. Unit-weighted cycles gave R_1 = 0.029 and R_2 = 0.029 for 2415 reflections. Similar unit-weighted refinement cycles with the more complete ($2\theta_{MoK\bar{\alpha}}$ < 54.9°) data set gave R_1 = 0.038 and R_2 = 0.037 for 3486 reflections. The final cycles of empirically weighted[14] full-matrix least-squares refinement with 62 independent atoms gave R_1 = 0.037 and R_2 = 0.038 for 3486 independent reflections having $2\theta_{MoK\bar{\alpha}}$ < 54.9° and $I > 3\sigma(I)$.

All structure factor calculations utilized the atomic form factors compiled by Cromer and Mann,[15] an anomalous dispersion correction[16] to the scattering factor of the Fe and P atoms, and a least-squares refinable extinction correction.[17] The computer programs used for these calculations are listed in ref 12.

Results and Discussion

Nitrile Derivatives of $Fe_3(\mu_3\text{-}PC_6H_5)_2(CO)_9$ and $Co_4(\mu_4\text{-}PC_6H_5)_2(CO)_{10}$. Acetonitrile and propionitrile cleanly displaced one carbonyl ligand in $Fe_3(\mu_3\text{-}PC_6H_5)_2(CO)_9$, **1**, at temperatures of 60–80 °C to form $Fe_3(\mu_3\text{-}PC_6H_5)_2(CO)_8(NCR)$, **2**. A bis(acetonitrile) derivative, $Fe_3(\mu_3\text{-}PC_6H_5)_2(CO)_7(NCR)_2$, **3**, was generated by photolysis of **1** in acetonitrile solution. Consistently, the mono(acetonitrile) derivative was converted to the bis complex on photolysis in acetonitrile. The structure and dynamic stereochemistry of these nitrile complexes are described in the following sections.

Although the parent cluster **1** underwent no ligand substitution reactions at 25 °C, the nitrile derivatives **2** and **3** did. The nitrile ligands in **2** and **3** were readily displaced by a variety of molecules that included nitriles, carbon monoxide, trimethyl phosphite, triphenylphosphine, phosphorus trifluoride, and triphenylarsine, and the resultant $Fe_3(\mu_3\text{-}PC_6H_5)_2(CO)_8L$ and $Fe_3(\mu_3\text{-}PC_6H_5)_2(CO)_7L_2$ complexes were obtained in good yields. Nitrile exchange between $Fe_3(\mu_3\text{-}PC_6H_5)_2(CO)_8(NCCH_3)$ and propionitrile was fast with a reaction half-life of ~ 30 min. Curiously, the displacement of acetonitrile by trimethyl phosphite was slower (in toluene solution); the half-life of $Fe_3(\mu_3\text{-}PC_6H_5)_2(CO)_8(NCCH_3)$ in the presence of a five fold excess of trimethyl phosphite was greater than 2 h. Possibly, the substitution reactions of these nitrile derivatives either are not mechanistically analogous or are not simply dissociative (nitrile dissociation) in character. Nevertheless, the iron atom substitution site is maintained in all the nitrile displacement reactions.

Acetonitrile displacement of one carbonyl ligand also occurred thermally in $Co_4(\mu_4\text{-}PC_6H_5)_2(CO)_{10}$, **4**, to give $Co_4(\mu_4\text{-}PC_6H_5)_2(CO)_9(NCCH_3)$, **5**. The latter complex, like the analogous iron complex, reacted with a variety of molecules like CO, $P(OCH_3)_3$ and $P(C_6H_5)_3$ to form the corresponding $Co_4(\mu_4\text{-}PC_6H_5)_2(CO)_9L$

(9) See paragraph at end of paper regarding supplementary material.

(10) "International Tables for X-Ray Crystallography"; Knyoch Press: Birmingham, England, 1974; Vol. IV, pp 55–66.

(11) "International Tables for X-Ray Crystallography"; Kynoch Press: Birmingham, England, 1969; Vol. I: (a) p 151; (b) p 119.

(12) Wreford, S. S.; Kouba, J. K.; Kirner, J. F.; Muetterties, E. L.; Tavanaiepour, I.; Day, V. W. *J. Am. Chem. Soc.* **1980**, *102*, 1558.

(13) The R values are defined as $R_1 = \sum||F_o| - |F_c||/\sum|F_o|$ and $R_2 = \{\sum w(|F_o| - |F_c|)^2/\sum w|F_o|^2\}^{1/2}$, where w is the weight given each reflection. The function minimized is $\sum w(|F_o| - K|F_c|)^2$, where K is the scale factor.

(14) Empirical weights were calculated from the equation $\sigma = \sum^3{}_0 a_n|F_o|^n = 2.43 - 2.39 \times 10^{-2}|F_o| + 1.64 \times 10^{-4}|F_o|^2 - 1.50 \times 10^{-7}|F_o|^3$, the a_n being coefficients derived from the least-squares fitting of the curve $||F_o| - |F_c| = \sum^3{}_0 a_n|F_o|^n$, where the F_c values were calculated from the fully refined model using unit weighting and an $I > 3\sigma(I)$ rejection criterion.

(15) Cromer, D. T.; Mann, J. L. *Acta Crystallogr., Sect. A* **1968**, *A24*, 324.

(16) Cromer, D. T. *Acta Crystallogr.* **1965**, *18*, 17.

(17) Zachariasen, W. H. *Acta Crystallogr.* **1967**, *23*, 558.

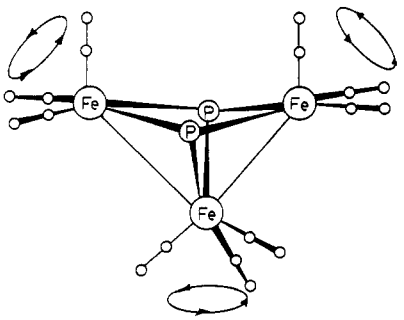

Figure 1. Illustrated above is the basic cluster structure for $Fe_3(\mu_3\text{-}PC_6H_5)_2(CO)_9$. The phenyl substituents on the phosphorus atoms are not depicted and the open circles for the ligands on the iron atoms represent carbon and oxygen atoms of CO. The three circles with arrows schematically illustrate the specific processes that contribute to the overall stereochemical nonrigidity of this molecule. These processes comprise CO site exchange localized on individual iron atoms. There was no fast CO intermetal site exchange between iron atoms discernible by NMR spectroscopy.

complexes under conditions where the parent cluster 4 underwent substitution at a substantially lower rate.

Stereochemistry of $Fe_3(\mu_3\text{-}PC_6H_5)_2(CO)_8L$ Complexes. $Fe_3(\mu_3\text{-}PC_6H_5)_2(CO)_9$, as crystallographically defined by Dahl and Huntsman[18] and by Cook et al.,[19] has a square-pyramidal array of three iron and two phosphorus atoms (Figure 1), with two equivalent and trans oriented basal iron atoms and a unique axial iron atom. Carbonyl ligands in the cluster are partitioned into four stereochemical groups: six basal Fe–CO of axial and equatorial configuration and two different apical Fe–CO orientations. Given this configurational complexity in the parent molecule 1, derivatives might exist in solution as a number of isomers. In order to define solution state stereochemistry, ^{13}CO-enriched 1 was prepared by utilizing the lability of the acetonitrile derivative 2. Subsequently, 1-^{13}*CO* was used through nitrile substitution to prepare ^{13}C CO-enriched phosphine, arsine, and phosphite derivatives.

The ^{13}C NMR spectrum (−60 °C) of ^{13}CO-enriched $Fe_3(\mu_3\text{-}PC_6H_5)_2(CO)_9$ consisted of three resonances at −214.4, −213.7, and −206.4 ppm which respectively can be assigned, based on integrated intensities, to apical iron $Fe(CO)_3$, basal iron Fe(CO) of axial form, and basal iron $Fe(CO)_2$ of equatorial form (see Figures 1 and 2). At higher temperatures, carbonyl site exchange occurred at localized basal iron sites whereby axial and equatorial CO site exchange was fast. Carbonyl site exchange between apical and basal iron atoms was not detectable on the NMR time scale. The inequivalence of apical iron–carbonyl sites, as established crystallographically,[7] was not discernible at −60 °C in the ^{13}C NMR spectrum, a not unexpected feature in view of the nominal seven-coordinate character of the apical iron atoms.

Assuming that the above assignment is correct, resonances can be assigned for ^{13}CO-enriched phosphine-, phosphite-, and arsine-substituted clusters on the basis of chemical shifts, phosphorus–phosphorus spin–spin coupling constants, and relative intensities. $Fe_3(\mu_3\text{-}PC_6H_5)_2(CO)_8(NCC_2H_5)$ displayed a simple AB pattern in the ^{31}P NMR, indicating that substitution was stereospecific and disymmetric with respect to the phosphorus caps. The ^{13}C NMR of the enriched sample was consistent with this. At low temperatures (Figure 3), one apical iron ^{13}CO resonance of relative intensity 3, two basal iron axial ^{13}CO resonances each of intensity 1, and two basal iron equatorial ^{13}CO resonances of intensity 2 and 1 were observed. These data incisively established that nitrile substitution is at an equatorial basal iron position. At high temperatures, axial–equatorial carbonyl site exchange centered at the unsubstituted basal iron was fast but no ligand site exchange centered at the substituted basal iron atom was detected.

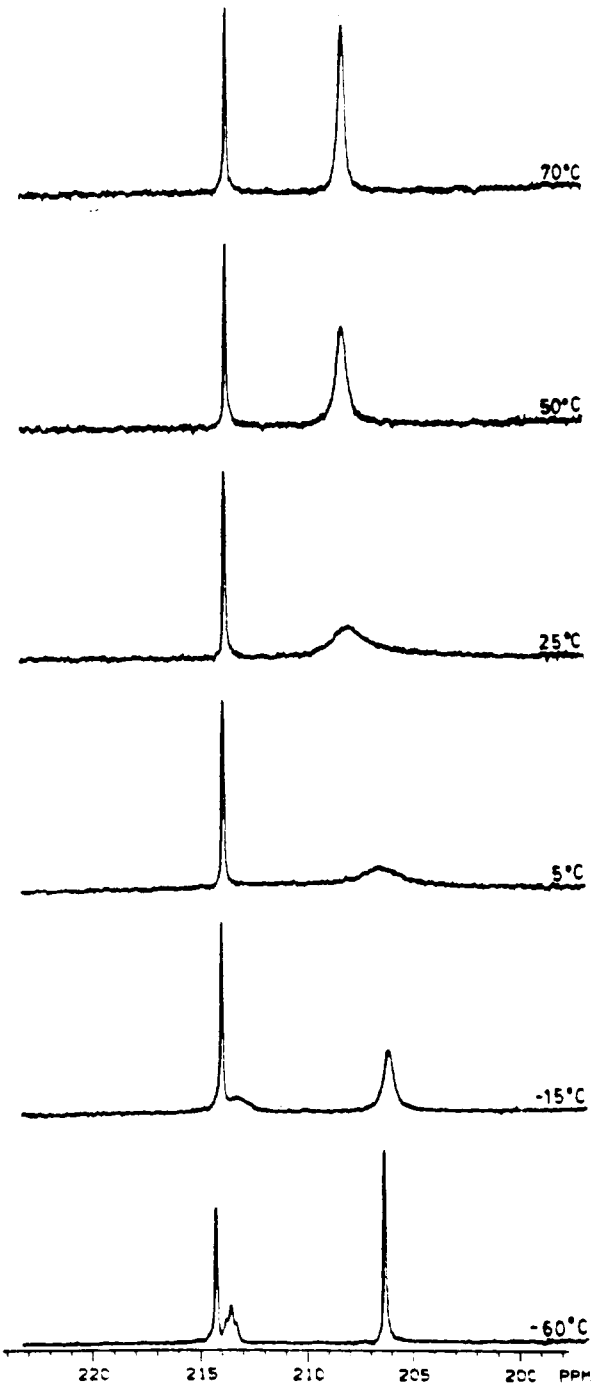

Figure 2. The stereochemical nonrigidity of $Fe_3(\mu_3\text{-}PC_6H_5)_2(CO)_9$ was established by a ^{13}C CO DNMR study. The results are illustrated above. The invariant resonance near −214.4 ppm is assigned to the time-averaged CO groups bonded to the apical iron atom. Carbonyl groups bonded to basal iron atoms give rise to the two resonances observed at low temperatures—the axial set at ~213.7 ppm (triplet fine structure due to ^{31}P–^{13}C coupling) and the equatorial set at ~−206 ppm (see Figure 1). Carbonyl group site exchange between the axial and equatorial conformational positions was rapid above −50 °C leading to collapse of these resonances to a single peak above 25 °C.

The structural dynamics of $Fe_3(\mu_3\text{-}PC_6H_5)_2(CO)_8L$ clusters where L is $P(OCH_3)_3$, $P(C_6H_5)_3$, and $As(C_6H_5)_3$ appeared to be identical so only the trimethyl phosphite example is discussed here. At room temperature, the ^{1}H NMR spectrum of $Fe_3(\mu_3\text{-}PC_6H_5)_2(CO)_8[P(OCH_3)_3]$ showed two types of trimethyl phosphite resonances, indicating the presence of two isomers. The low-temperature ^{31}P NMR of the cluster consisted of a single A_2B pattern indicating the presence of a single isomer which is symmetrically substituted with respect to the phosphorus capping

(18) Huntsman, J. R. Ph.D. Thesis, University of Wisconsin, Madison, 1973.
(19) Cook, S. L.; Evans, J.; Gray, L. R.; Webster, M. *J. Organomet. Chem.* **1982**, *236*, 367.

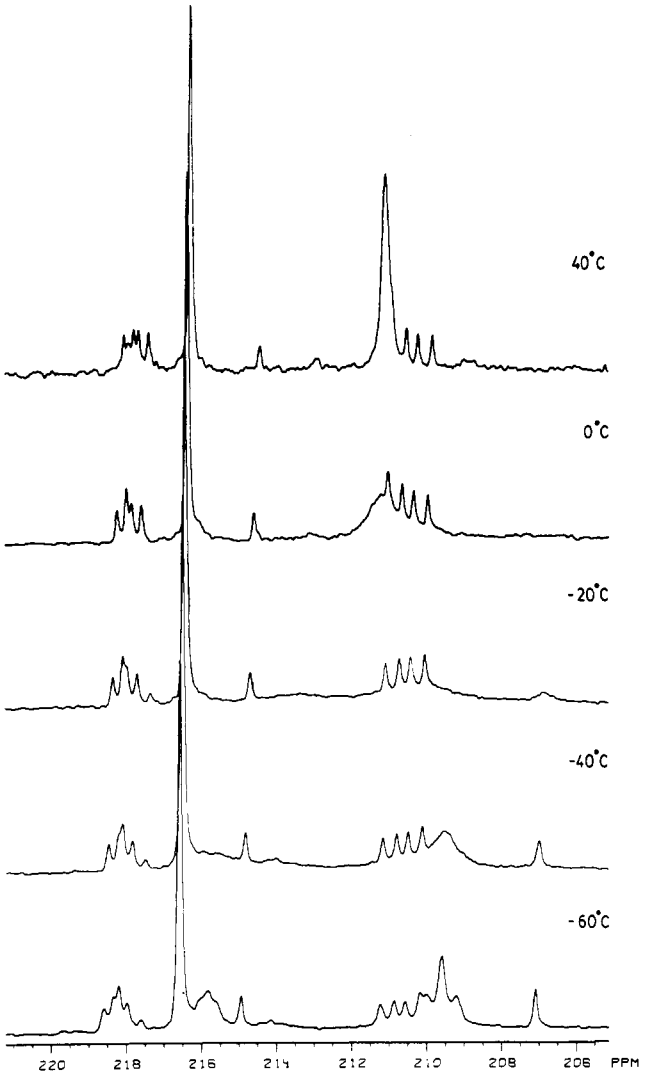

Figure 3. Shown above are the ^{13}C CO DNMR spectra for $Fe_3(\mu_3\text{-}PC_6H_5)_2(CO)_8(NCC_2H_5)$. The relatively sharp, essentially temperature invariant peak at ~−216.5 ppm arises from the apical iron $Fe(CO)_3$ group. The doublet of doublets at −218.2 and −210.7 ppm at −60 °C are assigned respectively to the axial and the basal CO ligands bonded to the basal iron that has an equatorial CH_3CN ligand. The multiplet at ~−216 ppm and the triplet at −209.6 at −60 °C are respectively assigned to the axial and basal CO ligands at the unsubstituted basal iron atom; only this set of distinguishable CO sites undergo fast (NMR timescale) at elevated temperatures as shown by the collapse of these resonances into a single peak above −20 °C.

atoms. At higher temperatures, the A_2B pattern collapsed and then reformed as an A_2B pattern with a different J_{AB} coupling constant. These spectral changes are consistent with the interconversion of two isomers, one of which predominates at low temperatures. The ^{13}C NMR of the enriched sample clearly supported this interpretation. At low temperatures, the spectrum was consistent with the presence of a single isomer substituted axially on a basal iron in that one axial CO and two equatorial basal Fe CO resonances were observed in addition to the apical iron CO resonance. At higher temperatures, CO exchange was observed between axial and equatorial sites on the unsubstituted basal iron. Thus, $Fe_3(\mu_3\text{-}PC_6H_5)_2(CO)_8L$ clusters, L = $P(OCH_3)_3$, $P(C_6H_5)_3$, and $As(C_6H_5)_3$, exist as solution state equilibrium mixtures of basal iron Fe–L conformational isomers of axial and equatorial form, with axial form favored, probably for steric reasons, whereas $Fe_3(\mu_3\text{-}PC_6H_5)_2(CO)_8(NCCH_3)$ apparently exists as a single isomer with the nitrile bonded to a basal iron atom in an equatorial site. The iron atom site of substitution is preserved in the conversion of the nitrile to the phosphite, phosphine, and arsine derivatives.

Table I. Atomic Coordinates for Non-Hydrogen Atoms in Crystalline $Fe_3(\mu_3\text{-}PC_6H_5)_2(CO)_7(NCCH_3)$

atom type[b]	fractional coordinates 10^4x	10^4y	10^4z	equiv isotropic thermal parameter B,[c] Å^2
		Molecule a		
Fe_1	3801.6 (7)	2500.0 (. . .)[d]	961.6 (3)	3.0
Fe_2	5916.4 (7)	2500.0 (. . .)[d]	891.4 (4)	3.3
Fe_3	5733.9 (8)	2500.0 (. . .)[d]	1957.9 (4)	3.5
P	4877.4 (9)	3250.8 (7)	1387.7 (4)	3.2
N	3252 (3)	3319 (2)	479 (1)	3.7
O_{11}	2305 (4)	2500 (. . .)[d]	1802 (2)	5.4
O_{21}	5212 (4)	2500 (. . .)[d]	−216 (2)	5.1
O_{22}	7370 (3)	3813 (3)	870 (2)	6.5
O_{31}	4372 (5)	2500 (. . .)[d]	2877 (2)	7.6
O_{32}	7179 (3)	3758 (2)	2229 (2)	6.2
C_{11}	2863 (5)	2500 (. . .)[d]	1448 (3)	3.6
C_{21}	5451 (5)	2500 (. . .)[d]	228 (3)	3.8
C_{22}	6805 (4)	3299 (3)	868 (2)	4.7
C_{31}	4914 (7)	2500 (. . .)[d]	2518 (3)	5.1
C_{32}	6618 (4)	3273 (3)	2127 (2)	4.5
C_1	2879 (4)	3780 (3)	229 (2)	4.4
C_2	2379 (10)	4388 (5)	−94 (5)	7.0
C_{p1}	4849 (3)	4324 (3)	1391 (2)	3.6
C_{p2}	4701 (4)	4726 (3)	1864 (3)	5.1
C_{p3}	4653 (5)	5566 (4)	1849 (4)	5.8
C_{p4}	4805 (5)	5951 (4)	1382 (4)	6.6
C_{p5}	4977 (5)	5561 (4)	924 (4)	6.2
C_{p6}	4996 (5)	4740 (3)	926 (3)	5.2
		Molecule b		
Fe_1	267.7 (7)	2500 (. . .)[d]	−1760.9 (4)	3.2
Fe_2	−70.8 (7)	2500 (. . .)[d]	−669.9 (4)	3.8
Fe_3	−2018.6 (7)	2500 (. . .)[d]	−1001.1 (4)	3.3
P	−767.9 (9)	3251.0 (7)	−1310.3 (4)	3.1
N	1317 (3)	3304 (2)	−1896 (1)	3.8
O_{11}	−902 (4)	2500 (—)[d]	−2736 (2)	5.9
O_{21}	2141 (4)	2500 (. . .)[d]	−758 (3)	7.0
O_{22}	−326 (4)	3823 (3)	69 (2)	8.1
O_{31}	−3325 (5)	2500 (. . .)[d]	−1938 (2)	6.2
O_{32}	−2868 (3)	3783 (2)	−355 (1)	5.3
C_{11}	−395 (5)	2500 (. . .)[d]	−2362 (3)	3.9
C_{21}	1258 (6)	2500 (. . .)[d]	−743 (3)	4.8
C_{22}	−219 (5)	3313 (4)	−214 (2)	5.8
C_{31}	−2832 (5)	2500 (. . .)[d]	−1563 (3)	4.1
C_{32}	−2551 (4)	3282 (3)	−602 (2)	4.1
C_1	1932 (4)	3747 (3)	−1979 (2)	4.6
C_2	2720 (8)	4324 (7)	−2087 (6)	7.7
C_{p1}	−807 (3)	4318 (3)	−1329 (2)	3.4
C_{p2}	−1712 (4)	4710 (3)	−1443 (2)	4.2
C_{p3}	−1736 (5)	5527 (3)	−1485 (2)	4.8
C_{p4}	−856 (5)	5954 (3)	−1422 (3)	5.2
C_{p5}	42 (5)	5579 (3)	−1303 (2)	5.2
C_{p6}	72 (4)	4759 (3)	−1258 (2)	4.5

[a] Figures in parentheses are the estimated standard deviations in the last significant digit. [b] Atoms are labeled in agreement with Figure 4. [c] All non-hydrogen atoms are modeled with anisotropic thermal parameters of the form $\exp[-(\beta_{11}h^2 + \beta_{22}k^2 + \beta_{33}l^2 + 2\beta_{12}hk + 2\beta_{13}hl + 2\beta_{23}kl)]$; this is the equivalent isotropic thermal parameter calculated from $B = 4[V^2 \det(\beta_{ij})]^{1/3}$. [d] This is a symmetry-required value and is listed without an estimated standard deviation.

$Fe_3(\mu_3\text{-}PC_6H_5)_2(CO)_8(PF_3)$ was prepared and studied by ^{19}F, ^{31}P, and ^{13}C NMR. The presence of two isomers at low temperatures was established by the ^{19}F and ^{31}P NMR data. At higher temperatures, the resonances associated with the one isomer began to coalesce but not with the resonances of the second, detectable isomer. These data indicate the presence of three isomers: an apical $FePF_3$ derivative which does not equilibrate with basal $FePF_3$ isomers on the NMR time scale, a basal $FePF_3$ derivative of axial form, and a trace amount of basal $FePF_3$ derivative of equatorial form. The ^{13}C NMR data supported the proposed presence of an apically substituted isomer. The presence of an

Table IV. Bond Lengths (Å) in Crystalline $Fe_3(\mu_3\text{-}PC_6H_5)_2(CO)_7(NCCH_3)_2$[a]

type[b]	molecule a	molecule b	av[c]	type[b]	molecule a	molecule b	av[c]
Fe_1-Fe_2	2.776 (1)	2.768 (1)	2.772 (1, 4)	P-C_{p1}	1.822 (5)	1.812 (5)	1.817 (5, 5)
Fe_2-Fe_3	2.681 (1)	2.684 (1)	2.683 (1, 2)	N-C_1	1.115 (5)	1.121 (6)	1.118 (6, 3)
$Fe_1 \cdots Fe_3$	3.554 (1)	3.549 (1)	3.552 (1, 3)	C_1-C_2	1.465 (9)	1.449 (9)	1.457 (9, 8)
Fe_1-P	2.179 (2)	2.177 (1)	2.178 (1, 1)	C_{p1}-C_{p2}	1.382 (7)	1.390 (6)	
				C_{p1}-C_{p6}	1.372 (7)	1.385 (7)	
Fe_2-P	2.241 (1)	2.243 (2)	2.242 (1, 1)	C_{p2}-C_{p3}	1.429 (10)	1.392 (8)	1.381 (8, 20, 48, 12)
				C_{p3}-C_{p4}	1.355 (11)	1.370 (8)	
Fe_3-P	2.218 (1)	2.216 (1)	2.217 (1, 1)	C_{p4}-C_{p5}	1.341 (11)	1.370 (8)	
				C_{p5}-C_{p6}	1.394 (8)	1.397 (8)	
Fe_1-N	1.978 (4)	1.967 (4)	1.973 (4, 6)				
Fe_1-C_{11}	1.731 (7)	1.737 (7)	1.734 (7, 3)	C_2-H_{21}	0.83 (9)	0.76 (7)	
				C_2-H_{22}	0.83 (6)	0.98 (11)	
Fe_2-C_{21}	1.770 (7)	1.750 (9)	1.781 (7, 18, 31, 8)	C_2-H_{23}	0.83 (8)	0.87 (7)	
Fe_2-C_{22}	1.788 (5)	1.801 (6)		C_{p2}-H_{p2}	0.94 (4)	0.81 (4)	0.89 (7, 8, 13, 10)
Fe_3-C_{31}	1.767 (9)	1.766 (7)		$C_{p3}H_{p3}$	0.88 (6)	0.95 (5)	
Fe_3-C_{32}	1.801 (5)	1.803 (5)		$C_{p4}H_{p4}$	1.00 (8)	0.97 (6)	
				C_{p5}-H_{p5}	0.95 (6)	0.92 (5)	
C_{11}-O_{11}	1.148 (7)	1.149 (8)		C_{p6}-H_{p6}	0.90 (4)	0.88 (5)	
C_{21}-O_{21}	1.156 (7)	1.158 (9)					
C_{22}-O_{22}	1.145 (6)	1.129 (6)					
C_{31}-O_{31}	1.145 (9)	1.140 (8)		P$\cdots$P	2.549 (3)	2.549 (2)	2.549 (3, 0)
C_{32}-O_{32}	1.133 (6)	1.130 (5)					

[a] Figures in parentheses following an individual entry are the estimated standard deviation in the last significant digit. [b] Atoms are labeled in agreement with Figure 4. [c] See ref 20.

apically substituted isomer is not surprising considering the chemical similarity between CO and PF_3. Reaction of ^{13}CO with basal-substituted $Fe_3(\mu_3\text{-}PC_6H_5)_2(CO)_8(CH_3CN)$ gave a statistical distribution of ^{13}CO at each site of the product $Fe_3(\mu_3\text{-}PC_6H_5)_2(CO)_9$.

The ^{31}P NMR spectrum of the bis(nitrile) cluster consisted of a single resonance, indicating either symmetrical substitution or fast exchange between unsymmetric isomers. The ^{13}C NMR of a ^{13}CO-enriched sample showed one apical iron carbonyl resonance of intensity 3, two axial basal iron carbonyl resonances, each of intensity 1, and a single basal iron equatorial carbonyl resonance of intensity 2. Only one of the axial carbonyl ligands exchanged with the equatorial carbonyl groups at higher temperatures. These data indicated that both CH_3CN ligands are equatorially oriented on the same basal iron atom. This supposition was confirmed by the X-ray crystallographic study reported below. The only other structurally characterized bis(acetonitrile) cluster derivative is $Os_4(\mu\text{-}H)_3(CO)_{12}(NCCH_3)_2^+$ which has the nitrile ligands on different metal atoms.[2a]

$Fe_3(\mu_3\text{-}PC_6H_5)_2(CO)_7[P(OCH_3)_3]_2$ was prepared from the bis(nitrile) complex. All four phosphorus atoms were shown to be inequivalent by ^{31}P NMR. A temperature dependence of the ^{31}P resonances was observed in which coupling constants changed, but this process did not equilibrate phosphite sites or PC_6H_5 phosphorus sites. This temperature dependence was limited to *one* of the phosphite phosphorus atoms and both PC_6H_5 phosphorus atoms. The inequivalence of all phosphorus atoms is consistent with a structure in which both phosphite ligands are on the same basal iron atom (consistent with the stereochemistry of the bis acetonitrile precursor complex). We have no unique interpretation of the marked temperature dependence of the chemical shifts.

Molecular Structure of $Fe_3(\mu_3\text{-}PC_6H_5)_2(CO)_7(NCCH_3)_2$, 3. The X-ray structural analysis established that single crystals of $Fe_3(\mu_3\text{-}PC_6H_5)_2(CO)_7(NCCH_3)_2$ are composed of discrete triiron cluster molecules which possess rigorous C_s-m symmetry. Final atomic coordinates and anisotropic thermal parameters for non-hydrogen atoms of **3** are given with estimated standard deviations in Tables I and II,[9] respectively. Atomic coordinates and isotropic thermal parameters for hydrogen atoms of **3** are given in Table III.[9] Bond lengths and angles for **3** are given in Tables IV and V, respectively.

The asymmetric unit for crystalline **3** contains two crystallographically independent $Fe_3(\mu_3\text{-}PC_6H_5)_2(CO)_7(NCCH_3)_2$ molecules (designated a and b, respectively). An ORTEP drawing of the first (a) molecule is shown in Figure 4; the second (b) molecule differs principally in a slight (~11.4)° rotation of the phenyl ring about

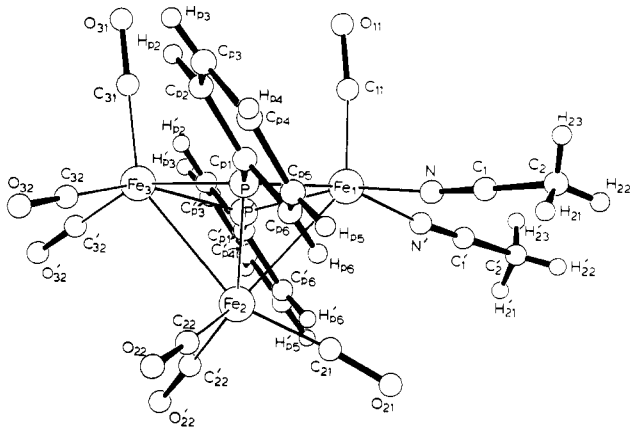

Figure 4. Perspective drawing (adapted from an ORTEP plot) of the solid-state structure for one (molecule a) of the two crystallographically independent $Fe_3(\mu_3\text{-}PC_6H_6)_2(CO)_7(NCCH_3)_2$ molecules, **3**. Both molecules possess crystallographic C_s-m symmetry. Atoms labeled with a prime (′) are related to those without by the crystallographic mirror plane at $(x, {}^1/_4, z)$ in the unit cell which contains Fe_1, Fe_2, Fe_3, C_{11}, O_{11}, C_{21}, O_{21}, C_{31}, and O_{31}. For purposes of clarity, the Fe and P atoms are represented by large circles; O, N, and C atoms are represented by medium-sized circles and H atoms by small circles. The second molecule (b) differs from this one principally in a slight (~11.4°) rotation of the phenyl rings about the P–C bonds.

the P–C vector. These triiron clusters are very similar to the parent $Fe_3(\mu\text{-}PC_6H_5)_2(CO)_9$ molecule **1** and are electron precise if the Fe_1–Fe_2 and Fe_2–Fe_3 vectors which have average lengths of 2.772 (1, 4, 4, 2) Å and 2.683 (1, 2, 2, 2) Å,[20] respectively, represent single-order metal–metal bonds and the 3.552 (1, 3, 3, 2) Å-$Fe_1 \cdots Fe_3$ separation represents a nonbonded interaction.

Since the structure of **3** is very similar to that of the previously described[18,19] parent **1**, we will restrict ourselves to comparisons between them. Structurally, **3** can be derived from **1** by replacing the two equatorial CO ligands on a single basal Fe by two ace-

(20) The first number in parenthesis following an averaged value of a bond length or angle is the root-mean-square estimated standard deviation of an individual datum. The second and third numbers, when given, are the averge and maximum deviations from the averaged value, respectively. The fourth number represents the number of individual measurements which are included in the average value.

Table V. Bond Angles (deg) in Crystalline $Fe_3(\mu_3\text{-}PC_6H_5)_2(CO)_7(NCCH_3)_2$[a]

type[b]	molecule a	molecule b
PFe_1P'	71.57 (7)	71.68 (7)
PFe_3P'	70.12 (7)	70.23 (7)
PFe_1Fe_2	52.08 (4)	52.30 (4)
PFe_3Fe_2	53.43 (4)	53.46 (4)
PFe_1C_{11}	96.6 (2)	97.9 (2)
PFe_3C_{31}	101.8 (2)	99.6 (2)
PFe_1N	97.1 (1)	96.8 (1)
PFe_3C_{32}	93.4 (2)	93.2 (2)
PFe_1N'	161.0 (1)	158.7 (1)
PFe_3C_{32}'	153.6 (2)	154.6 (2)
Fe_2Fe_1N	108.9 (1)	106.4 (1)
$Fe_2Fe_3C_{32}$	100.2 (2)	101.3 (2)
$Fe_2Fe_1C_{11}$	138.9 (2)	140.8 (2)
$Fe_2Fe_3C_{31}$	147.7 (2)	145.1 (2)
$C_{11}Fe_1N$	99.9 (2)	101.6 (2)
$C_{31}Fe_3C_{32}$	101.7 (2)	102.1 (2)
NFe_1N'	89.3 (2)	87.8 (2)
$C_{32}Fe_3C_{32}'$	93.5 (3)	94.9 (3)
PFe_2Fe_1	50.10 (4)	50.17 (4)
PFe_2Fe_3	52.66 (4)	52.53 (4)
PFe_2P'	69.31 (7)	69.26 (7)
PFe_2C_{21}	108.1 (2)	109.3 (2)
PFe_2C_{22}	89.0 (2)	88.5 (2)
PFe_2C_{22}'	147.7 (2)	147.6 (2)
$Fe_1Fe_2Fe_3$	81.25 (4)	81.22 (4)
$C_{21}Fe_2C_{22}$	101.2 (2)	99.6 (2)
$C_{22}Fe_2C_{22}'$	98.6 (4)	100.0 (4)
$C_{21}Fe_2Fe_1$	73.5 (2)	74.8 (2)
$C_{21}Fe_2Fe_3$	154.7 (2)	156.0 (2)
$C_{22}Fe_2Fe_1$	130.7 (2)	130.0 (2)
$C_{22}Fe_2Fe_3$	95.2 (2)	95.4 (2)
$C_{p1}PFe_1$	125.3 (2)	126.2 (2)
$C_{p1}PFe_2$	125.4 (2)	126.7 (2)
$C_{p1}PFe_3$	125.3 (2)	124.2 (2)
Fe_1PFe_3	107.84 (5)	107.78 (5)
Fe_1PFe_2	77.81 (5)	77.52 (5)
Fe_2PFe_3	73.91 (5)	74.01 (5)
$PC_{p1}C_{p2}$	119.9 (4)	120.5 (4)
$PC_{p1}C_{p6}$	120.5 (4)	120.9 (4)
$C_{p2}C_{p1}C_{p6}$	119.5 (5)	118.5 (5)
$C_{p1}C_{p2}C_{p3}$	118.5 (7)	120.8 (5)
$C_{p2}C_{p3}C_{p4}$	119.8 (7)	119.9 (5)
$C_{p3}C_{p4}C_{p5}$	121.7 (7)	120.2 (5)
$C_{p4}C_{p5}C_{p6}$	119.6 (8)	120.3 (6)
$C_{p5}C_{p6}C_{p1}$	121.0 (7)	120.3 (5)
Fe_1NC_1	174.9 (5)	178.1 (7)
NC_1C_2	179.2 (9)	179.5 (13)
$Fe_1C_{11}O_{11}$	174.3 (7)	174.7 (7)
$Fe_2C_{21}O_{21}$	175.6 (6)	176.0 (7)
$Fe_2C_{22}O_{22}$	177.9 (5)	179.0 (11)
$Fe_3C_{31}O_{31}$	179.1 (14)	177.5 (10)
$Fe_3C_{32}O_{32}$	179.3 (12)	178.5 (8)
$C_{p1}C_{p2}H_{p2}$	121 (3)	124 (3)
$C_{p3}C_{p2}H_{p2}$	121 (3)	115 (3)
$C_{p2}C_{p3}H_{p3}$	106 (5)	117 (3)
$C_{p4}C_{p3}H_{p3}$	134 (5)	123 (3)
$C_{p3}C_{p4}H_{p4}$	122 (4)	121 (3)
$C_{p5}C_{p4}H_{p4}$	116 (4)	118 (4)
$C_{p4}C_{p5}H_{p5}$	122 (4)	123 (4)
$C_{p6}C_{p5}H_{p5}$	118 (4)	117 (4)
$C_{p5}C_{p6}H_{p6}$	120 (3)	120 (3)
$C_{p1}C_{p6}H_{p6}$	119 (3)	120 (3)
$C_1C_2H_{21}$	117 (7)	111 (6)
$C_1C_2H_{22}$	111 (6)	130 (7)
$C_1C_2H_{23}$	111 (5)	106 (5)
$H_{21}C_2H_{22}$	114 (7)	114 (8)
$H_{21}C_2H_{23}$	100 (8)	115 (8)
$H_{22}C_2H_{23}$	102 (6)	74 (7)

[a] Figures in parentheses following an individual entry are the estimated standard deviation in the last significant digit.
[b] Atoms are labeled in agreement with Figure 4.

Table VI. M-$NCCH_3$ Bond Distance (Å) and Angle (deg) Data for Nitrile Derivatives of Metal Clusters

complex	M-N	N-C	M-N-C	ref
$Os_3(CO)_{11}(NCCH_3)$	2.074 (23)	1.246 (44)	173.6 (17)	2c
$Os_3(CO)_{10}(NCCH_3)_2$	2.122 (15)	1.121 (23)	176.7 (16)	2c
	2.133 (13)	1.112 (22)	169.9 (14)	
$Os_3(CO)_{10}(NCCH_3)(CON_3C_6H_5)$	2.083 (15)	1.113 (25)	176.4 (12)	21b, 24
$Ru_5C(CO)_{15}(NCCH_3)$	2.119 (15)	1.101 (24)	171.0 (16)	21a, 24
$(CH_3CN)_2Cu_2Ru_6C(CO)_{16}$	1.906 (4)	1.123 (6)	174.9 (5)	4c
	1.907 (5)	1.122 (6)	167.6 (5)	
$(CH_3CN)_2Cu_2Rh_6(CO)_{15}\cdot 0.5CH_3OH$	1.90 (1)	1.12 (1)	178 (10)	4b
$Fe_3(\mu_3\text{-}PC_6H_5)_2(CO)_7(NCCH_3)_2$	1.978 (4)	1.115 (5)	174.9 (5)	this work
	1.967 (4)	1.121 (6)	178.1 (7)	
$Fe_3(CO)_9(\mu_3\text{-}\eta^2\text{-}NCCH_2CH_2CH_3)$	1.795 (2)	1.260 (3)	160.0 (2)	5a
	1.974 (2)			

tonitrile ligands. Carbon monoxide and acetonitrile are both formally two-electron donor ligands when terminally bonded to a single transition metal, but they have very different π-acceptor properties. These differences in acceptor capability are probably responsible for the structural differences between 1 and 3. Although molecules of 1 have no crystallographically imposed symmetry in the solid state, the square-pyramidal Fe_3P_2 cores of both crystallographically independent molecules approximate

C_{2v} symmetry. Molecules of **3** possess crystallographic C_s-m symmetry in the solid but their Fe_3P_2 cores do not approximate C_{2v} symmetry. The Fe–P bonds to basal iron atoms Fe_1 and Fe_3 in **1** are equivalent and have an average value of 2.216 (5, 8, 17, 8) Å[19,20] which is quite similar to the 2.198 (1, 20, 21, 4)-Å average for the corresponding Fe–P bonds in **3**. The Fe_1–P and Fe_3–P bonds in **3** are not equivalent because they are trans to ligands with considerably different π-acceptor properties: Fe_1 had acetonitrile ligands trans to the two cis bridging phosphorus atoms and Fe_3 has a carbonyl ligand trans to them. Thus, the cis phosphorus atoms in **3** are competing with carbonyl ligands on Fe_3 and acetonitrile ligands on Fe_1 for back-donation of electron density from the same metal orbital. The observed 0.039-Å shortening of the Fe_1–P bonds in **3** relative to the Fe_3–P bonds is thus consistent with carbonyl being the better π-acceptor ligand. The presence of two relatively poor π-acceptor acetonitrile ligands on Fe_1 should also make it electron rich relative to Fe_3 and could explain the 0.032-Å shortening of the Fe_1–C_{11} bond relative to Fe_3–C_{31} through enhanced metal→ligand π bonding. Such an enhancement of metal–ligand π bonding for C_{11} could explain the 0.089-Å elongation of the Fe_1–Fe_2 bonds in **3** relative to Fe_2–Fe_3. The Fe_1–Fe_2 and Fe_2–Fe_3 bonds are equivalent in **1**[19] and have an average value of 2.717 (3, 1, 3, 4) Å[20] which is comparable to the 2.727 (1, 45, 49, 4)-Å average value in **3**. Similar effects have been observed in other metal cluster molecules containing acetonitrile and carbonyl ligands bonded to the same metal.[2a,c,21]

The remainder of the bond lengths and angles for **3** are unexceptional.[22] Note that the Fe–N bonds to the nitrile ligand average to 1.973 (4, 6, 6, 2) Å, which is close to the 2.00-Å sum of the respective covalent radii, and that the nitrile C–N bonds in **3** average to 1.118 (6) Å which compares with a range of 1.11 (2)–1.25 (4) Å established for terminally bonded acetonitrile in other metal complexes.[1c,4] Consistent with the weak character of the iron–nitrile bond, no elongation of the nitrile bond was detectable: the 1.118 (6) Å distance in the complexed nitrile is essentially indistinguishable from the 1.158 (2) Å value for free alkyl cyanides.[23]

Listed in Table VI are M–N and N–C distances and the M–N–C bond angles in nitrile derivatives of cluster molecules. The significant features of these parameters are the nearly linear M–N–C angles for terminally bound nitrile ligands and the close correspondence (within experimental error) in N–C distances between the free nitrile and the bound nitrile (terminally bound). However, in $Fe_3(CO)_9(\mu_3\text{-}\eta^2\text{-}NCCH_2CH_2CH_3)$ where both the nitrogen and the carbon atoms of the NC group are bonded to metal atoms, the N–C distance is significantly increased (1.260 (30) Å vs. 1.118 (6) Å for free alkyl cyanides).

Acknowledgment. This research was supported by the National Science Foundation. Some of the DNMR studies were performed by Dr. Robert R. Burch. We thank Dr. P. R. Raithby for detailed crystallographic data on nitrile cluster derivatives.[2,21,24]

Registry No. **1**, 38903-71-8; **2** (R = CH_3), 86372-86-3; **2** (R = C_2H_5), 86372-87-4; **3** (R = CH_3), 86372-88-5; **3** (R = C_2H_5), 86372-89-6; **4**, 58092-22-1; **5**, 86372-90-9; $Fe_3(PC_6H_5)_2(CO)_8[P(OCH_3)_3]$ (isomer 1), 86420-08-8; $Fe_3(PC_6H_5)_2(CO)_8[P(OCH_3)_3]$ (isomer 2), 86420-09-9; $Fe_3(PC_6H_5)_2(CO)_8[As(C_6H_5)_3]$ (isomer 1), 86372-92-1; $Fe_3(PC_6H_5)_2(CO)_8[As(C_6H_5)_3]$ (isomer 2), 86420-10-2; $Fe_3(PC_6H_5)_2(CO)_8[P(C_6H_5)_3]$ (isomer 1), 86372-93-2; $Fe_3(PC_6H_5)_2(CO)_8[P(C_6H_5)_3]$ (isomer 2), 86420-11-3; $Fe_3(PC_6H_5)_2(CO)_8(PF_3)$ (isomer 1), 86372-94-3; $Fe_3(PC_6H_5)_2(CO)_8(PF_3)$ (isomer 2), 86373-01-5; $Fe_3(PC_6H_5)_2(CO)_8(PF_3)$ (isomer 3), 86420-12-4; $Fe_3(PHC_6H_5)_2(CO)_6$, 39049-79-1; $Fe_3(PC_6H_5)_2(CO)_7[P(OCH_3)_3]_2$, 86391-87-9; $Co_4(PC_6H_5)_2(CO)_9[P(OCH_3)_3]$, 86372-99-8; $Co_4(PC_6H_5)_2(CO)_8[P(OCH_3)_3]_2$, 86373-00-4; $Co_4(PC_6H_5)_2(CO)_9[P(C_6H_5)_3]$, 86372-91-0; $Fe_3(PC_6H_5)_2(^{13}CO)_9$, 86372-95-4; $Fe_3(PC_6H_5)_2(^{13}CO)_8(NCC_2H_5)$, 86372-96-5; $Fe_3(PC_6H_5)_2(^{13}CO)_7(NCCH_3)_2$, 86372-97-6; $Fe_3(PC_6H_5)_2(^{13}CO)_8[P(OCH_3)_3]$, 86372-98-7; $N_{92}Fe(CO)_4$, 14878-31-0; $Na_2Fe_2(CO)_8$, 64913-30-0; $Co_2(CO)_8$, 10210-68-1; Fe, 7439-89-6; Co, 7440-48-4; $C_6H_5PCl_2$, 644-97-3; CH_3CN, 75-05-8; $NCCH_2CH_3$, 107-12-0; $P(OMe)_3$, 121-45-9; $As(C_6H_5)_3$, 603-32-7; $P(C_6H_5)_3$, 603-35-0; PF_3, 7783-55-3; HCl, 7647-01-0; ^{13}CO, 1641-69-6; iron pentacarbonyl, 13463-40-6.

Supplementary Material Available: Crystal structure analysis report, Tables II and III, positional and thermal parameters for non-hydrogen atoms and refined hydrogen atom positions for **3**, and structure factor tables (24 pages). Ordering information is given on any current masthead page.

(21) (a) Johnson, B. F. G.; Lewis, J.; Nicholls, J. N.; Oxton, I. A.; Raithby, P. R.; Rosales, M. J. *J. Chem. Soc., Chem. Commun.* **1982**, 289. (b) Burgess, K.; Johnson, B. F. G.; Lewis, J.; Raithby, P. R. *J. Chem. Soc., Dalton Trans.* **1982**, 2119.

(22) There were no intermolecular contacts significantly less than the corresponding van der Waals values.

(23) "Interatomic Distances 1960-65"; Crystallographic Data Centre: Cambridge, 1972; Vol. A1, p 52.

(24) Raithby, P. R., private communication.

The Role of Acetyl Complexes in the Cobalt-Catalyzed Homologation of Methanol

Jeffrey T. Martin and Michael C. Baird*

Department of Chemistry, Queen's University, Kingston, Ontario, Canada K7L 3N6

Received February 3, 1983

It is shown that stoichiometric hydrogenation of $MeCOCo(CO)_3PMePh_2$ in methanol yields a product distribution similar to that obtained during the homologation of methanol catalyzed by $[Co(CO)_3PMePh_2]_2$. The result suggests that the acetyl compound is an intermediate during the catalytic reaction.

Introduction

Much of the current interest in transition-metal-catalyzed reactions of synthesis gas is derived from the impending need to find new processes for the conversion of coal to feedstocks for the organic chemical industry.[1,2] Of great potential importance[3,4] is the alcohol homologation reaction, in which an alcohol, RCH_2OH, is converted to its next higher homologue, i.e., eq 1. This cobalt carbonyl catalyzed reaction was first reported in 1949[5] but elicited

(1) Falbe, J., Ed. "New Syntheses with Carbon Monoxide"; Springer-Verlag: New York, 1980.

(2) Falbe, J., Ed. Chemical Feedstocks from Coal; Wiley: New York, 1982.

(3) Bahrmann, H.; Cornils, B., ref 1, p 226.

(4) Cornils, B.; Rottig, W., ref 2, p 477.

0276-7333/83/2302-1073$01.50/0